

## Investigations on the electrochemical properties of new conjugated polymers containing benzo[*c*]cinnoline and oxadiazole moieties

Jyh-Chien Chen<sup>a,\*</sup>, Hsin-Chung Wu<sup>a</sup>, Chi-Jui Chiang<sup>a</sup>, Li-Chia Peng<sup>a</sup>, Tuo Chen<sup>a</sup>, Li Xing<sup>b</sup>, Shun-Wei Liu<sup>c</sup>

<sup>a</sup> Department of Materials Science and Engineering, National Taiwan University of Science and Technology, No. 43, Sec. 4, Keelung Rd., Taipei 10607, Taiwan

<sup>b</sup> Pfizer Worldwide Research and Development, 200 Cambridge Park Drive, Cambridge, MA 02140, USA

<sup>c</sup> Department of Electronic Engineering, Mingchi University of Technology, No. 84, Gongzhuang Rd., New Taipei City 24301, Taiwan

### ARTICLE INFO

#### Article history:

Received 26 August 2011  
Received in revised form  
28 October 2011  
Accepted 31 October 2011  
Available online 4 November 2011

#### Keywords:

Electrochemical properties  
Oxadiazole  
Benzo[*c*]cinnoline

### ABSTRACT

A four-step route was designed to synthesize 3,8-benzo[*c*]cinnoline dicarboxylic acid (**4**). New conjugated polymers, **POXD (I)** and **POXD (T)**, containing benzo[*c*]cinnoline and oxadiazole moieties, were obtained by thermal cyclodehydration of their soluble polyhydrazide precursors **PHA (I)** and **PHA (T)**, respectively. Two reduction peaks were observed for these new conjugated polymers during CV cathodic scan. From the CV voltammograms combined with the results from molecular simulation, we concluded that the first reduction occurred at oxadiazole moiety and benzo[*c*]cinnoline moiety was responsible for the second reduction. It indicates that oxadiazole has stronger electron affinity than benzo[*c*]cinnoline. We proposed a mechanism to explain this two-stage reduction process. Due to the planar and electron-accepting ability of benzo[*c*]cinnoline and oxadiazole moieties, **POXD (I)** and **POXD (T)** exhibited very low LUMO (−3.42 and −3.45 eV) and HOMO (−6.23 and −6.27 eV) energy levels. They can be used as hole-blocking or electron-injection layers for OLED applications.

© 2011 Elsevier Ltd. All rights reserved.

### 1. Introduction

Conjugated polymers have been attracting intensive research activities because of their versatile applications for organic light-emitting diodes (OLEDs) [1–4], photovoltaic cells [5–8] and thin film transistors [9]. In comparison to their inorganic counterparts, conjugated polymers can be solution (ink-jet) processable, and manufactured at relatively low costs. Furthermore, their chemical structures can be designed by organic reactions to meet the various requirements, resulting in the abundance of new conjugated polymers. However, most conjugated polymers such as poly(*p*-phenylenevinylene)s (PPVs) [10], poly(*p*-phenylene)s (PPPs) [11], poly(thiophene)s (PTs) [12], poly(fluorene)s (PFs) [13] and their derivatives [14,15] are  $\pi$ -electron excessive (electron-rich) in nature and hence have better hole-injection and hole-transporting ability [16,17]. As a result, the imbalanced hole and electron mobility could lead to poor performance of the organic electronic devices. In addition, the adjustments of HOMO, LUMO energy levels and band gaps are also critical for conjugated polymers to be applied in multi-layered or bulk hetero-junction devices. It has been reported that the incorporation of strong electron affinity (EA) moieties into

conjugated polymers can effectively improve the electron mobility, lower LUMO, HOMO energy levels and in some cases decrease the energy gaps once donor-acceptor pair is formed [18–20]. Several structures with strong electron affinity (electron-accepting) have been investigated, including 2,1,3-benzothiadiazole [7], pyridine [21], quinoxaline [18], cyanovinylene [22], 1,3,4-oxadiazole [23], 2,2'-bis(trifluoromethyl)biphenyl [24] and others. However, compared to the numerous literatures focused on electron-rich conjugated polymers, the reports on the new moieties with strong electron affinity are relatively rare. PBD(2-(4-biphenyl)-5-(4-*tert*-butylphenyl)-1,3,4-oxadiazole) was the first documented electron-transporting material used in a double layer OLED, which showed lower turn-on voltage and higher electroluminescence efficiency [25]. 1,3,4-Oxadiazole moiety has also been introduced in main chains or side chains of various conjugated polymers [26–28]. The resulted oxadiazole-containing conjugated polymers improved device performance. The poor solubility of poly(1,3,4-oxadiazole)s, resulted from the planar and rigid oxadiazole heterocycles, was generally circumvented by preparing their soluble polyhydrazide precursors first, followed by thermal cyclodehydration.

Benzo[*c*]cinnoline and its derivatives are planar, nitrogen-containing heterocyclic moieties. They have been reported as physiologically active molecules [29]. The nitrogen atoms at 5 and 6 positions are strongly electron-attracting that may dramatically affect the reactivity of the substituted functional

\* Corresponding author. Tel.: +886 2 27376526; fax: +886 2 27376544.  
E-mail address: [jcchen@mail.ntust.edu.tw](mailto:jcchen@mail.ntust.edu.tw) (J.-C. Chen).

group on the ring. The HOMO and LUMO energy levels of benzo[c]cinnoline molecule were reported to be lower than those of their carbon-containing counterparts [30]. Therefore, it can be expected that benzo[c]cinnoline can be a potential electron-accepting moiety. In this study, as the first part of our serious efforts on incorporation of benzo[c]cinnoline ring into various conjugated polymers, poly(1,3,4-oxadiazole)s containing benzo[c]cinnoline moiety were prepared via their polyhydrazide precursors followed by thermal cyclodehydration. Their electrochemical properties were investigated by cyclic voltammetry (CV). A mechanism to explain the observed two-stage reduction (CV cathodic scan) was proposed according to the results from molecular simulation. We concluded that the oxadiazole had stronger electron affinity than benzo[c]cinnoline. The possible applications for OLEDs were also discussed.

## 2. Experimental

### 2.1. Materials

Tetrabutylammonium perchlorate (TBAP) used in cyclic voltammetric measurements was recrystallized twice with ethyl acetate and dried at 120 °C under reduced pressure overnight. All of the other reagents were purchased from commercial companies and used as received. All of the solvents used in this study were purified according to standard methods prior to use.

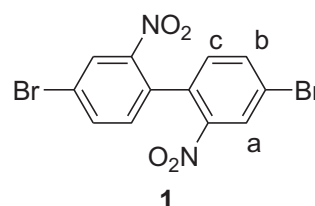
### 2.2. Measurements

All melting points were determined on a Mel-Temp capillary melting point apparatus. Proton ( $^1\text{H}$  NMR) and carbon ( $^{13}\text{C}$  NMR) nuclear magnetic resonance spectra were measured at 500 and 125 MHz on a Bruker Avance-500 spectrometer, respectively. Infrared spectra were obtained with a Digilab-FTS1000 FTIR. Mass spectroscopy was conducted on a Finnigan TSQ 700 mass spectrometer. Inherent viscosities were determined with a Cannon-Ubbelohde No. 100 viscometer at  $30.0 \pm 0.1$  °C. Molecular weights were measured on a JASCO GPC system (PU-980) equipped with an RI detector (RI-930), a Jordi Gel DVB Mixed Bed column (250 mm  $\times$  10 mm), using dimethylacetamide (DMAc) as the eluent and calibrated with polystyrene standards. Thermal gravimetric analyses (TGA) were performed in nitrogen with a TA TGA Q500 thermogravimetric analyzer using a heating rate of 10 °C  $\text{min}^{-1}$ . Differential scanning calorimetry (DSC) measurements were carried out under  $\text{N}_2$  atmosphere using a Perkin–Elmer DSC 4000 analyzer at a heating rate of 20 °C/min. UV–vis spectrometry was carried out on a Cary-100 UV–vis spectrometer. Photoluminescence (PL) measurements were carried out on a Perkin–Elmer F4500 photoluminescence spectrometer. PL quantum yield ( $\Phi_{\text{PL}}$ ) of the polymer in concentrated sulfuric acid was measured by using  $10^{-5}$  M quinine sulfate in 1 N  $\text{H}_2\text{SO}_4$  as reference standard ( $\Phi_{\text{PL}} = 0.546$ ). Cyclic voltammetric (CV) measurements were carried out on a CH Instrument 611C electrochemical analyzer at room temperature in a three-electrode electrochemical cell with a working electrode (polymer film coated on ITO glass), a reference electrode ( $\text{Ag}/\text{Ag}^+$ , referenced against ferrocene/ferrocium ( $\text{Fc}/\text{Fc}^+$ ), 0.09 V), and a counter electrode (Pt gauze) at a scan rate of 100  $\text{mV s}^{-1}$ . CV measurements for polymer films were performed in an electrolyte solution of 0.1 M tetrabutylammonium perchlorate (TBAP) in acetonitrile. The potential window at oxidative scan was 0–2.5 V and reductive scan was 0~ –2.5 V, respectively. Wide-angle X-ray diffraction (WXRd) measurements were performed using polymer powder on a Rigaku TTRAX III with 18 kw rotation anode Cu target.

### 2.3. Synthesis of monomers

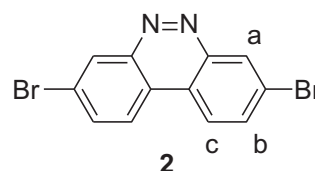
#### 2.3.1. 4,4'-Dibromo-2,2'-dinitrobiphenyl (1)

To a 250-mL, three-necked, round-bottomed flask equipped with a condenser were added 2,5-dibromonitrobenzene (11.43 g, 40.70 mmol), dimethylformamide DMF (77 mL) and activated copper powder (8.22 g, 129.45 mmol). The mixture was heated at 120 °C for 3 h under nitrogen atmosphere. After cooled to room temperature, the reaction mixture was added toluene (150 mL) and filtered. The clear filtrate was collected, washed with brine and water, dried over anhydrous  $\text{MgSO}_4$ . The solvent was evaporated. The crude solid was recrystallized from ethanol/toluene (4:1) to afford 5.73 g (70% yield) of light yellow crystals. mp 149–151 °C (lit [31], mp 149 °C).  $^1\text{H}$  NMR (500 MHz,  $\text{DMSO}-d_6$ ,  $\delta$ , ppm): 8.44 (d,  $J = 2.0$  Hz, 2H, Ar- $\text{H}_a$ ), 8.08 (dd,  $J_1 = 8.2$  Hz,  $J_2 = 2.0$  Hz, 2H, Ar- $\text{H}_b$ ), 7.49 (d,  $J = 8.2$  Hz, 2H, Ar- $\text{H}_c$ ).



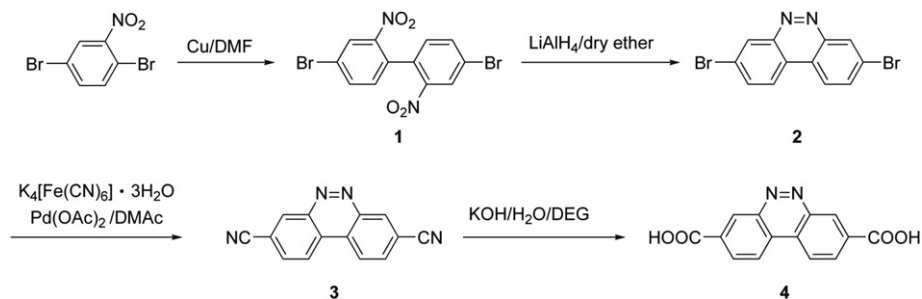
#### 2.3.2. 3,8-Dibromobenzo[c]cinnoline (2)

To a 500-mL, three-necked, round-bottomed flask equipped with a condenser was added  $\text{LiAlH}_4$  (1.80 g, 47.49 mmol) in anhydrous ether (70 mL) under nitrogen atmosphere. 4,4'-Dibromo-2,2'-dinitrobiphenyl (1) (2.40 g 6.00 mmol) in anhydrous ether (100 mL) and benzene (100 mL) was added into the reaction mixture. After stirred for 2 h at room temperature, the reaction mixture was heated at 45 °C for 15 min. Water (10 mL) was then slowly added to the reaction mixture to decompose excess  $\text{LiAlH}_4$ . The reaction mixture was filtered and solvents were evaporated. The yellow solid was collected and purified by column chromatography using dichloromethane as the eluent to afford 1.60 g (79% yield) of yellow needle-like crystals. mp 241–242 °C (lit [32], mp 242–243 °C).  $^1\text{H}$  NMR (500 MHz,  $\text{DMSO}-d_6$ ,  $\delta$ , ppm): 8.94 (d,  $J = 2.0$  Hz, 2H, Ar- $\text{H}_a$ ), 8.90 (d,  $J = 8.8$  Hz, 2H, Ar- $\text{H}_c$ ), 8.24 (dd,  $J_1 = 8.8$  Hz,  $J_2 = 2.0$  Hz, 2H, Ar- $\text{H}_b$ ). EIMS ( $m/z$ ): calcd. for  $\text{C}_{12}\text{H}_6\text{Br}_2\text{N}_2$ , 335.9; found, 335.9 [ $\text{M}^+$ ].



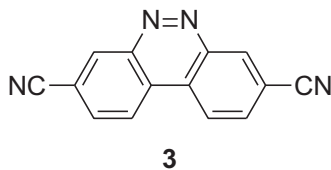
#### 2.3.3. 3,8-Dicyanobenzo[c]cinnoline (3)

To a 100-mL, three-necked, round-bottomed flask equipped with a condenser were added 3,8-dibromobenzo[c]cinnoline (2) (1.014 g, 3.00 mmol),  $\text{K}_4[\text{Fe}(\text{CN})_6] \cdot 3\text{H}_2\text{O}$  (0.557 g, 1.32 mmol),  $\text{Na}_2\text{CO}_3$  (0.636 g, 6.00 mmol), DMAc (20 mL), and  $\text{Pd}(\text{OAc})_2$  (0.005 g, 0.02 mmol). The flask was vacuumed and backfilled with  $\text{N}_2$  several times. The reaction mixture was heated at 120 °C under nitrogen atmosphere for 8 h. Ethyl acetate (50 mL) was then added to the reaction mixture when it was cooled to room temperature. The precipitate of the reaction mixture was collected by filtration and



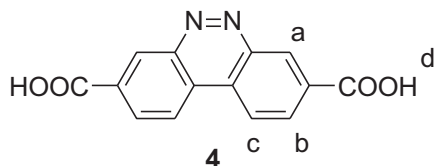
Scheme 1. Synthetic route for 3,8-benzo[c]cinnoline dicarboxylic acid (**4**).

washed with water, methanol (50 mL), dichloromethane (50 mL) and acetone (50 mL). The product was dried at 80 °C under reduced pressure for 12 h to afford 0.600 g (87% yield) of brown solid. The crude product was used for next step without further purification. mp >300 °C (decompose). EIMS ( $m/z$ ): calcd. for  $C_{14}H_6N_4$ , 230.0; found, 230.0 [ $M^+$ ].



#### 2.3.4. 3,8-Benzo[c]cinnoline dicarboxylic acid (**4**)

To a 100-mL, three-necked, round-bottomed flask equipped with a condenser were added crude 3,8-dicyanobenzo[c]cinnoline (**3**) (1.00 g, 4.35 mmol), diethylene glycol (20.0 mL), KOH (1.10 g, 19.60 mmol), and water (0.5 mL). The reaction mixture was heated at 220 °C for 12 h under nitrogen atmosphere. When the reaction mixture was cooled to room temperature, the precipitate that formed was collected and dissolved in hot water (250 mL). After filtration, the clear filtrate was acidified by concentrated HCl. The precipitate was collected and washed with water to afford 0.60 g (52% yield) of yellow solid. mp >300 °C (lit [33], mp 335 °C).  $^1H$  NMR (500 MHz,  $DMSO-d_6$ ,  $\delta$ , ppm): 13.71 (s, 2H, carboxylic acid- $H_d$ ), 9.19 (d,  $J = 1.6$  Hz, 2H, Ar- $H_a$ ), 9.06 (d,  $J = 8.5$  Hz, 2H, Ar- $H_c$ ), 8.53 (dd,  $J_1 = 8.5$  Hz,  $J_2 = 1.6$  Hz, 2H, Ar- $H_b$ ). EIMS ( $m/z$ ): calcd. for  $C_{14}H_8N_2O_4$ , 268.0; found, 267.9 [ $M^+$ ].



#### 2.4. Synthesis of polyhydrazide by direct polycondensation

##### 2.4.1. Polyhydrazide **PHA (I)**

To a 50-mL, round-bottomed, three-necked flask equipped with a mechanical stirrer, a condenser and a nitrogen inlet were added 3,8-benzo[c]cinnoline dicarboxylic acid (**4**) (0.268 g, 1.00 mmol), NMP (12.0 mL), LiCl (1.540 g), triphenyl phosphite (1.1 mL) and pyridine (2.9 mL). The reaction mixture was heated at 100 °C for 30 min under nitrogen atmosphere. Isophthalic dihydrazide (0.194 g, 1.00 mmol) was then added. The reaction mixture was heated at 140 °C for 6 h under nitrogen. After cooled to room temperature, the reaction mixture was poured into water (300 mL).

The precipitate that formed was collected and washed with water and hot methanol to afford 0.380 g (89% yield) of light green solid.

##### 2.4.2. Polyhydrazide **PHA (T)**

Polyhydrazide **PHA (T)** was prepared from 3,8-benzo[c]cinnoline dicarboxylic acid (**4**) and terephthalic dihydrazide using the same procedures for **PHA (I)** in 84% yield.

#### 2.5. Film preparation and thermal cyclodehydration of polyhydrazides

Polyhydrazides, **PHA (I)** and **PHA (T)** were dissolved in DMAc (0.05%, w/v). The formed polymer solutions were filtered through a syringe with a 0.45  $\mu$ m filter. The polymer solutions were spin-coated on a clean ITO glass which was then put in an air circulated oven at 100 °C for 1 h, 250 °C for 2 h, followed by 300 °C for 6 h under reduced pressure to afford polyoxadiazole films, **POXD (I)** and **POXD (T)**, respectively.

#### 2.6. Fabrication of electron-only devices

To fabricate the electron-only device for the current density investigation, a polyhydrazide solution (0.5%, w/v in *m*-cresol) was spin-coated on top of Al/glass substrate then converted to the corresponding polyoxadiazole by thermal cyclodehydration in vacuum. Aluminum tris(8-hydroxyquinolate) ( $Alq_3$ ) and Al electrode were then sequentially deposited through a shadow mask, giving an active device area of 0.2  $cm^2$ . The comparison device of  $Alq_3$  single layer was prepared identically. The devices were completed with an encapsulation in a glove box ( $O_2$  and  $H_2O$  concentration below 0.1 ppm). The evaporation rates of the organic

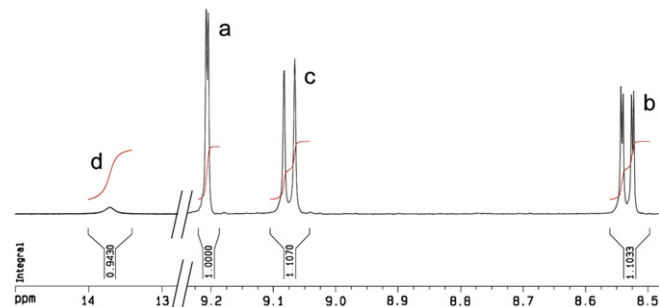
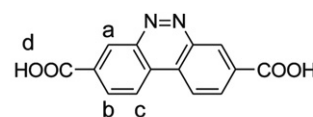
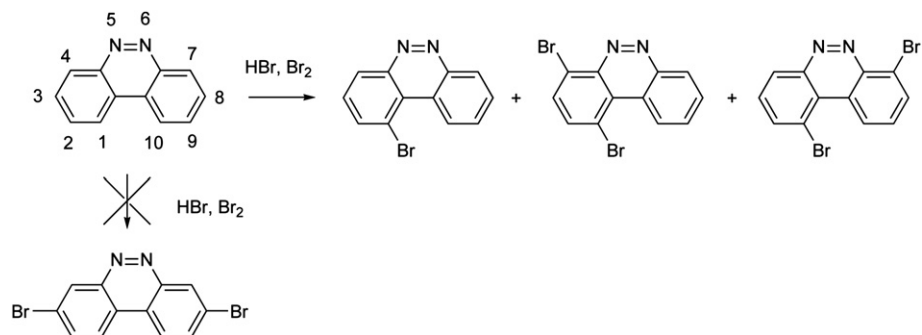


Fig. 1.  $^1H$  NMR spectrum of 3,8-benzo[c]cinnoline dicarboxylic acid (**4**) in  $DMSO-d_6$ .



**Scheme 2.** Direct bromination of benzo[c]cinnoline.

and metal layers were controlled to be 0.1 nm/s by quartz-crystal monitor and were calibrated by the thickness measurements with a surface profiler (150; Veeco Dektak). Subsequently, the electrical characteristics of each device were measured by a programmable dc power supply (2400; Keithley) in atmosphere at room temperature.

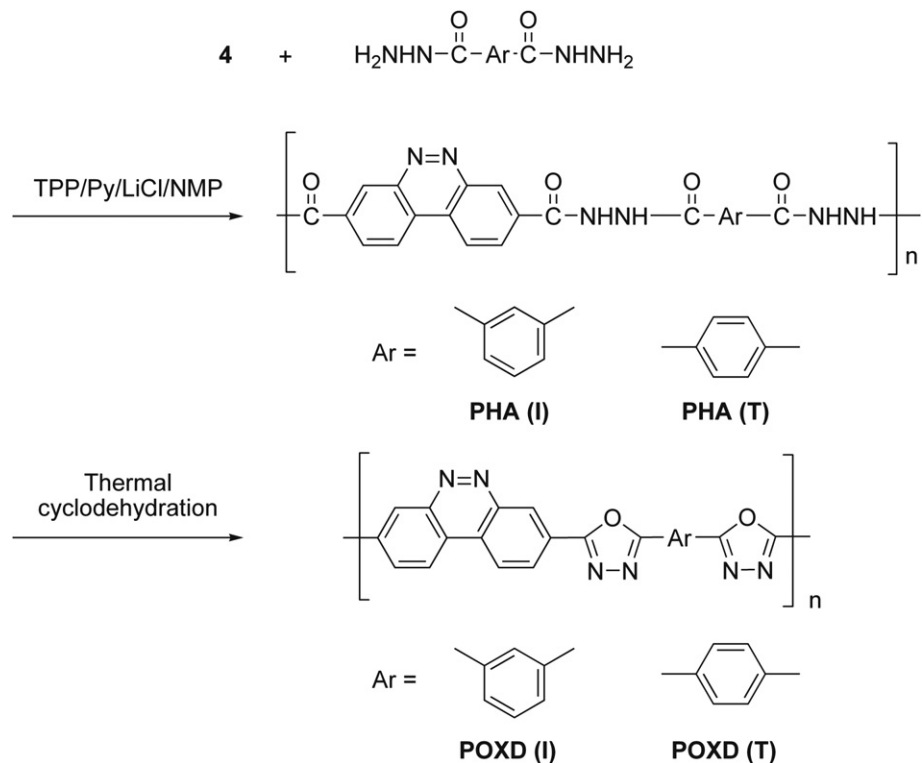
### 3. Results and discussion

#### 3.1. Synthesis of monomers

The diacid, 3,8-benzo[c]cinnoline dicarboxylic acid (**4**), was prepared by a four-step synthetic route as shown in Scheme 1. 2,5-Dibromonitrobenzene was first coupled by Ullmann coupling reaction to form 4,4'-dibromo-2,2'-dinitrobiphenyl (**1**). The dinitro compound (**1**) was then reduced by  $\text{LiAlH}_4$  to form 3,8-dibromobenzo[c]cinnoline (**2**). The bromide functional groups were converted to cyano groups. The final product, 3,8-benzo[c]cinnoline dicarboxylic acid (**4**) was obtained by the hydrolysis of dicyano compound (**3**). Fig. 1 shows the  $^1\text{H}$  NMR spectrum of 3,8-benzo[c]cinnoline dicarboxylic acid (**4**).

It was reported that direct bromination of benzo[c]cinnoline would lead to an isomeric mixture containing bromides on 1, or 1,4 or 1,7 positions as shown in Scheme 2 [34]. Therefore, 3,8-dibromobenzo[c]cinnoline (**2**) has to be prepared according to the proposed synthetic route (Scheme 1).

The dibromo functional groups of compound (**2**) can be polymerized or coupled with other moieties by Suzuki, Heck and Stille coupling reactions. If 2,5-dichloronitrobenzene is used as the starting material in Scheme 1, the formed 3,8-dichlorobenzo[c]cinnoline can under go aromatic nucleophilic substitution due to the electron-withdrawing benzo[c]cinnoline structure. In this study, we converted the bromides of compound (**2**) into cyano groups, which were further hydrolyzed to form 3,8-benzo[c]cinnoline dicarboxylic acid (**4**). Although it was reported that 3,8-benzo[c]cinnoline dicarboxylic acid (**4**) can be prepared by photochemical method or by acetophenone in the presence of alkoxide in alcoholic solvent, the yield was extremely low (9%) with tedious purification process and long reaction time (60 h) [33,35]. Our proposed synthetic route provided higher yield with easier workup procedures.



**Scheme 3.** Preparation of polyhydrazides and polyoxadiazoles.

**Table 1**  
Inherent viscosities and molecular weights of polyhydrazides and polyoxadiazoles.

Polymer	Yield	$M_n$ (g/mol) <sup>a</sup>	$\eta_{inh}$ (dL/g)	PDI <sup>a</sup>
<b>PHA (I)</b>	89%	6500	0.23 <sup>b</sup>	1.40
<b>PHA (T)</b>	84%	6000	0.20 <sup>b</sup>	1.35
<b>POXD (I)</b>	— <sup>d</sup>	—	0.27 <sup>c</sup>	—
<b>POXD (T)</b>	— <sup>d</sup>	—	0.15 <sup>c</sup>	—

<sup>a</sup> Obtained from GPC using DMAc as solvent and calibrated with polystyrene standards.

<sup>b</sup> Measured in NMP at 30 °C on 0.5 g dL<sup>-1</sup>.

<sup>c</sup> Measured in conc. H<sub>2</sub>SO<sub>4</sub> at 30 °C on 0.5 g dL<sup>-1</sup>.

<sup>d</sup> Quantitative yield in thermal cyclodehydration.

### 3.2. Synthesis of polymers

Polyhydrazides **PHA (I)** and **PHA (T)** were prepared by direct polycondensation (Scheme 3) from 3,8-benzo[*c*]cinnoline dicarboxylic acid (**4**) with isophthalic dihydrazide and terephthalic dihydrazide, respectively. Table 1 shows the inherent viscosities and molecular weights of these polymers. The inherent viscosities of **PHA (I)** and **PHA (T)** were 0.23 and 0.20 dL/g, measured in NMP at 30 °C with a concentration of 0.5 g/dL. The number average molecular weights ( $M_n$ ) were 6500 and 6000 g/mol measured by GPC in DMAc solvent. Polyoxadiazoles, **POXD (I)** and **POXD (T)**, were prepared by thermal cyclodehydration of their polyhydrazide precursors. After thermal cyclodehydration, the formed **POXD (I)** and **POXD (T)** were insoluble in any organic solvents. Their molecular weights can not be measured by GPC. The inherent viscosities of **POXD (I)** and **POXD (T)**, measured in concentrated sulfuric acid, were 0.27 and 0.15 dL/g, respectively.

These values (molecular weights and inherent viscosities) are not high when compared with those of other polyhydrazides and polyoxadiazoles. However, all of these polymers can form continuous, smooth, and pin-hole free films on ITO glass by spin coating process. The low molecular weights might be partly resulted from the low solid content (only 3%, w/v) we used during the direct polycondensation. In conventional direct polycondensation, the solid content was 7–8%, w/v [36]. For some monomers with ether or bulky pendant groups, the solid contents can be as high as 30%, w/v [37]. The higher solid content is beneficial to obtain polymers with high molecular weights. Due to the poor solubility resulted from the rigid and planar benzo[*c*]cinnoline structure, attempts to prepare **PHA (I)** and **PHA (T)** with solid contents higher than 3% would lead to precipitation during polymerization. Fig. 2 shows the

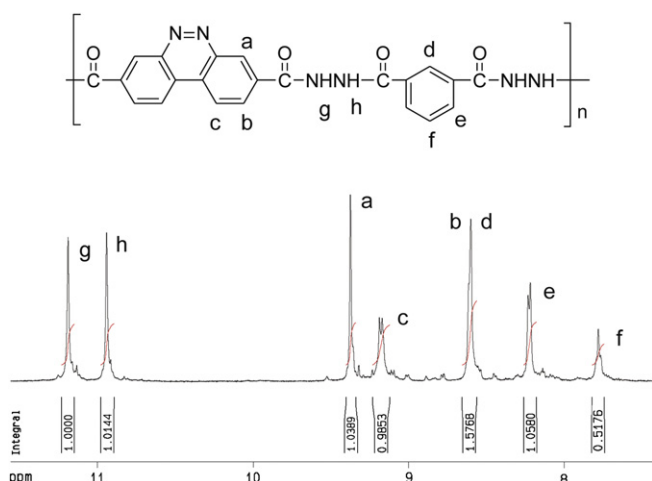


Fig. 2. <sup>1</sup>H NMR spectrum of **PHA (I)** in DMSO-*d*<sub>6</sub>.

**Table 2**  
Thermal properties of polyhydrazides and polyoxadiazoles.

Polymer	$T_d$ (°C) <sup>a</sup>	$T_g$ (°C) <sup>b</sup>	Char yield (wt%) <sup>c</sup>
<b>PHA (I)</b>	284	190	55
<b>PHA (T)</b>	292	210	60
<b>POXD (I)</b>	459	230	58
<b>POXD (T)</b>	469	250	59

<sup>a</sup> Measured by TGA at a heating rate of 10 °C/min in nitrogen.

<sup>b</sup> Measured by DSC at a heating rate of 20 °C/min in nitrogen.

<sup>c</sup> Residual weight percentage at 800 °C in nitrogen.

<sup>1</sup>H NMR spectrum of **PHA (I)**. Protons of hydrazide linkages appeared at 10.94 and 11.19 ppm. After thermal cyclodehydration, the IR absorption peaks at 3235 (N–H stretching) and 1655 (C=O stretching) cm<sup>-1</sup> disappeared and peaks attributed to the formation of oxadiazole ring, such as 1558 (C=N stretching) and 1077 (C–O–C stretching) cm<sup>-1</sup> appeared.

### 3.3. Thermal stability

The thermal stability was evaluated by the decomposition temperatures at 5% weight loss ( $T_d$ ) and glass transition temperatures ( $T_g$ ) as listed in Table 2. Fig. 3 shows the TGA thermograms of benzo[*c*]cinnoline-containing polyhydrazides and polyoxadiazoles. Two stages of weight loss were observed. The first stage was resulted from thermal cyclodehydration. The second stage was attributed to the decomposition of the formed polyoxadiazoles. The  $T_d$ s of **PHA (I)** and **PHA (T)** were 284 and 292 °C, respectively. The onset temperature of thermal cyclodehydration was around 280 °C. The  $T_d$ s of **POXD (I)** and **POXD (T)** were 459 and 469 °C, respectively. The  $T_g$ s of **PHA (I)** and **PHA (T)** were 190 and 210 °C. After thermal cyclodehydration, the  $T_g$ s of **POXD (I)** and **POXD (T)** were 230 and 250 °C. Polymers with *p*-catenation exhibited higher thermal stability than their *m*-catenated analogs. These values are comparable to those of conventional polyoxadiazoles. It indicates the good thermal stability of the benzo[*c*]cinnoline moiety.

### 3.4. Organo-solubility and crystallinity

The solubility was investigated at a concentration of 0.5%, w/v in various solvents. The results are summarized in Table 3. **PHA (I)** was soluble in all tested solvents except THF at room temperature, while *p*-catenated **PHA (T)** was only soluble in the same solvents at 60 °C.

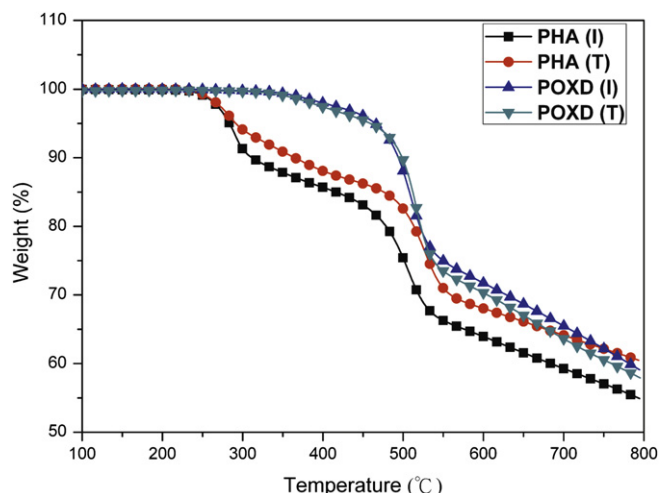


Fig. 3. TGA thermograms of polyhydrazides and polyoxadiazoles.

**Table 3**  
Solubility of polyhydrazides.<sup>a</sup>

Polymer	NMP	DMAc	DMF	DMSO	THF
PHA (I)	++	++	++	++	–
PHA (T)	+	+	+	+	–

Abbreviations: THF, tetrahydrofuran; DMF, dimethylformamide; DMAc, dimethylacetamide; NMP, *N*-methyl-2-pyrrolidinone; DMSO, dimethyl sulfoxide.

<sup>a</sup> Solubility was determined using 0.005 g of polymer in 1 mL of solvent. ++ (soluble at room temperature); + (soluble on heating at 60 °C); ± (partially soluble on heating at 60 °C); – (insoluble on heating at 60 °C).

After thermal cyclodehydration, the formed **POXD (I)** and **POXD (T)** were only soluble in concentrated sulfuric acid. This is resulted from the planar and rigid structures of benzo[*c*]cinnoline and oxadiazole as well.

Crystallinity was investigated by wide angle X-ray diffraction. Fig. 4 shows the diffraction patterns of these polymers. Polyhydrazides and polyoxadiazoles synthesized in this study all showed crystalline peaks. Previous studies have reported the amorphous character of polyhydrazides, which would become crystalline polyoxadiazoles after thermal cyclodehydration [37,38]. It was attributed to the formation of planar and rigid oxadiazole ring. In this study, the crystalline character of both polyhydrazides and polyoxadiazoles might be attributed to the presence of planar oxadiazole and benzo[*c*]cinnoline as well.

### 3.5. Optical properties

The UV–vis and photoluminescence (PL) spectra of these polymers ( $10^{-4}$ – $10^{-5}$  M in concentrated sulfuric acid) are shown in Fig. 5. Photoluminescence quantum yield was estimated using quinine sulfate as the standard. The data are summarized in Table 4. The maximum absorption wavelengths ( $\lambda_{\max}$ ) of **PHA (I)** and **PHA (T)** were at 265 and 269 nm, respectively. These wavelengths were red-shifted to 325 and 345 nm after the formation of **POXD (I)** and **POXD (T)**. The red shift could be attributed to the longer conjugated length after the formation of oxadiazole ring. This effect is more pronounced for *p*-catenated **POXD (T)** (76 nm) than for *m*-catenated **POXD (I)** (60 nm).

The photoluminescence (PL) spectra of **PHA (I)** and **PHA (T)** showed emission peaks at 453 and 456 nm, respectively. The emission peaks of **POXD (I)** and **POXD (T)** were at 459 and 472 nm.

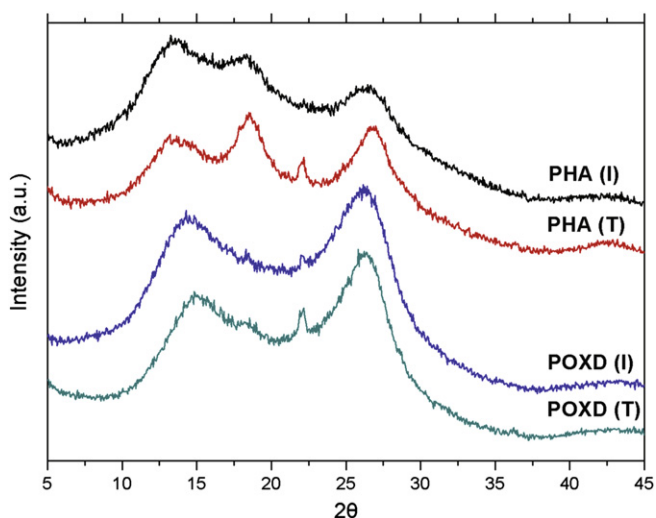


**Fig. 4.** Diffraction patterns of polyhydrazides and polyoxadiazoles.

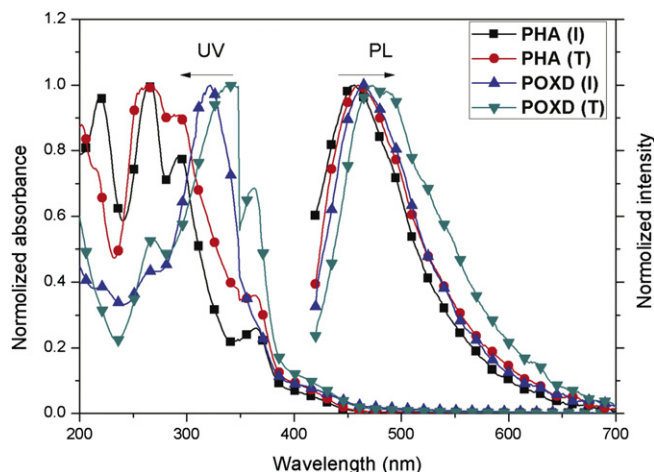


**Fig. 5.** UV–vis and PL spectra of polyhydrazides and polyoxadiazoles.

The similar red shifts of the emission peaks were observed after thermal cyclodehydration. The PL quantum yields of these new polymers ranged from 0.18 to 0.31%. These values are exceptionally low when compared with those of polyoxadiazole and its derivatives.

### 3.6. Electrochemical properties

The electrochemical redox behavior was characterized by cyclic voltammetry. Fig. 6 shows cyclic voltammograms (cathodic scan) of **PHA (I)**, **PHA (T)**, **POXD (I)** and **POXD (T)**. Polymer films remained stable during repeating scans and showed essentially the same cyclic voltammograms. No oxidation peak below 2.50 V was observed for **PHA (I)** and **PHA (T)**. The oxidation onset potentials of **POXD (I)** and **POXD (T)** were found to be 1.52 and 1.56 V, respectively. One irreversible reduction peak was observed for **PHA (I)** and **PHA (T)**. The reduction onset potentials ( $E_{\text{onset}}^{\text{red}}$ ) were at –1.53 and –1.64 V, respectively. This peak was attributed to the reduction of benzo[*c*]cinnoline moiety. After the formation of oxadiazole by thermal cyclodehydration, two irreversible reduction peaks were observed for **POXD (I)** and **POXD (T)**, respectively. For example, two reduction peaks with onset potentials of –1.26 and –1.55 V were found for **POXD (T)** as shown in Fig. 6. Comparing the cyclic voltammograms of polyhydrazides and polyoxadiazoles, we can reasonably assume that the first peak was attributed to the reduction of oxadiazole moiety and the second peak was the resulted from the reduction of benzo[*c*]cinnoline moiety. This implies that oxadiazole moiety had stronger electron affinity than benzo[*c*]cinnoline moiety.

To provide further evidence for the observed reduction behavior of these polymers, theoretical calculations were carried out with the Maestro graphical interface of Schrodinger molecular modeling

**Table 4**  
Optical properties of polyhydrazides and polyoxadiazoles.

Polymer	$\lambda_{\max}^{\text{UV}}$ (nm) <sup>a</sup>	$\lambda_{\max}^{\text{PL}}$ (nm) <sup>a</sup>	$\phi_{\text{PL}}$ (%) <sup>b</sup>
PHA (I)	265	453	0.20
PHA (T)	269	456	0.18
POXD (I)	325	459	0.31
POXD (T)	345	474	0.21

<sup>a</sup> Measured in conc.  $\text{H}_2\text{SO}_4$  with a concentration of  $10^{-4}$ – $10^{-5}$  M.

<sup>b</sup> PL quantum yields were estimated using quinine sulfate (dissolved in 1 N  $\text{H}_2\text{SO}_4(\text{aq})$ , assuming  $\phi_{\text{PL}}$  of 0.546) as a standard.

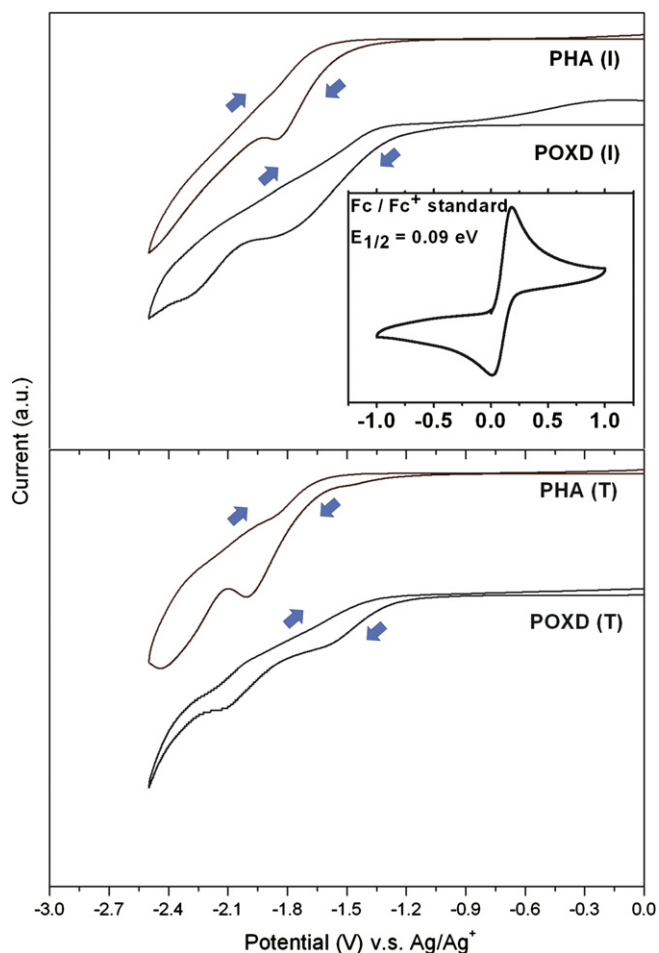


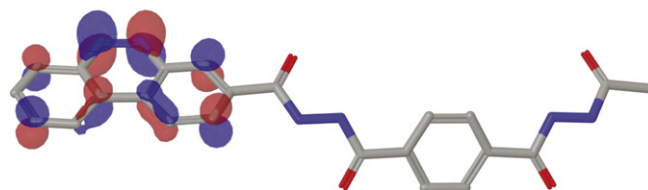
Fig. 6. Cyclic voltammograms (cathodic scan) of polyhydrazides and polyoxadiazoles.

suite (Maestro 9.1; Schrodinger, LLC: New York, 2010). The repeating units of **PHA (T)** and **POXD (T)** were employed in the molecular simulation. The details were described in the [Supplementary content](#). The simulated LUMOs of **PHA (T)** and **POXD (T)** are shown in Fig. 7(a) and (b), respectively. For **PHA (T)**, the LUMO is concentrated on the benzo[c]cinnoline moiety. In comparison, the LUMO of **POXD (T)** is distributed over the oxadiazoles and their conjugated benzene ring. Therefore the simulation suggests that the first electron addition (reduction) is most likely received by the oxadiazole ring. The LUMO was also calculated for the **POXD (T)** radical anion (charge =  $-1$ , spin multiplicity = 2) to predict the location of the second electron addition. Based on the results shown in Fig. 7(c), the second electron is added to the benzo[c]cinnoline moiety of **POXD (T)** radical anion.

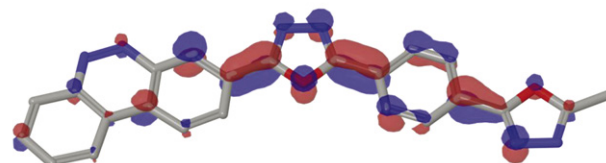
From the simulation results and the CV voltammograms of **PHA (T)** and **POXD (T)**, we concluded that during CV cathodic scan the first reduction peak was from oxadiazole moiety and the second reduction peak was from benzo[c]cinnoline moiety. Fig. 8 is our proposed mechanism to explain the reduction behavior of **POXD (T)** under CV cathodic scan.

The LUMO (electron affinity EA) and HOMO (ionization potential IP) energy levels were calculated from the onset potentials of reduction and oxidation, respectively. The absolute energy level of ferrocene/ferrocenium ( $\text{Fc}/\text{Fc}^+$ ) is assumed to be 4.8 eV below vacuum level. The external  $\text{Fc}/\text{Fc}^+$  redox standard  $E_{1/2}$  was determined to be 0.09 V versus  $\text{Ag}/\text{Ag}^+$  in acetonitrile by our

a LUMO of **PHA (T)**



b LUMO of **POXD (T)**



c LUMO of **POXD (T)** radical anion

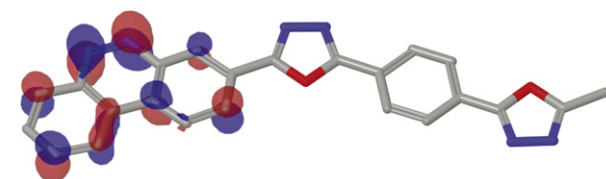


Fig. 7. Simulated LUMOs of (a) **PHA (T)**, (b) **POXD (T)**, and (c) **POXD (T)** radical anion.

electrochemical measuring system [39]. The results are summarized in Table 5. The calculated LUMO energy levels were  $-3.18$  and  $-3.07$  eV for **PHA (I)** and **PHA (T)**, respectively. The calculated LUMO and HOMO energy levels were  $-3.42$  and  $-6.23$  eV for **POXD (I)**,  $-3.45$  and  $-6.27$  eV for **POXD (T)**. The energy band gaps calculated from electrochemical measurement were 2.81 eV for **POXD (I)** and 2.82 eV for **POXD (T)**. The energy levels for various

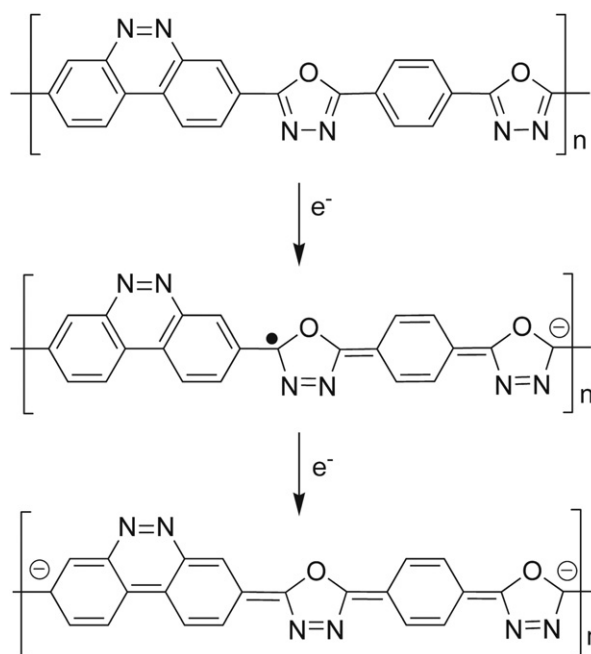


Fig. 8. Mechanism of **POXD (T)** reduction under CV cathodic scan.

**Table 5**  
Electrochemical properties of polyhydrazides and polyoxadiazoles.

Polymer	$E_{\text{onset}}^{\text{ox}}$ (V) <sup>a</sup>	$E_{\text{onset}}^{\text{red}}$ (V) <sup>a</sup>		$E_{\text{HOMO}}$ (eV)	$E_{\text{LUMO}}$ (eV) <sup>d</sup>	$E_{\text{g, ec}}$ (eV) <sup>e</sup>	$E_{\text{g, opt}}$ (eV) <sup>f</sup>
		1st	2nd				
<b>PHA (I)</b>		-1.53		-5.58 <sup>b</sup>	-3.18		2.67
<b>POXD (I)</b>	1.52	-1.29	-1.55	-6.23 <sup>c</sup>	-3.42	2.81	2.58
<b>PHA (T)</b>		-1.64		-5.77 <sup>b</sup>	-3.07		2.70
<b>POXD (T)</b>	1.56	-1.26	-1.55	-6.27 <sup>c</sup>	-3.45	2.82	2.64

<sup>a</sup> Measured by cyclic voltammetry.

<sup>b</sup>  $E_{\text{HOMO}} = E_{\text{LUMO}} - E_{\text{g, opt}}$ .

<sup>c</sup>  $E_{\text{HOMO}} = -(E_{\text{onset}}^{\text{ox}} + 4.80 - 0.09)$  (eV).

<sup>d</sup>  $E_{\text{LUMO}} = -(E_{\text{onset}}^{\text{red}} + 4.80 - 0.09)$  (eV).

<sup>e</sup>  $E_{\text{g, ec}} = \text{IP}(E_{\text{onset}}^{\text{ox}}) - \text{EA}(E_{\text{onset}}^{\text{red}})$  (eV).

<sup>f</sup> Calculated by the equation:  $1240/\lambda_{\text{onset}}$ .

organic materials including poly{5-methoxy-2-[(2'-ethylhexyloxy)-*p*-phenylenevinylene] (MEH-PPV) [40], aluminum tris(8-hydroxyquinolate) (Alq<sub>3</sub>) [41], cyano-substituted poly(*p*-phenylenevinylene) (CN-PPV) [40], 2-(4-biphenyl)-5-(4-*tert*-butylphenyl)-1,3,4-oxadiazole (PBD) [42], poly(*p*-phenylene-1,3,4-oxadiazole) (*p*-POD) [43], poly(pyridine-2,5-diyl) (PPy) [44], and poly(quinoxaline-5,8-diyl) (PQX) [45] are shown in Fig. 9. The benzo[*c*]cinnoline-containing polyoxadiazoles, **POXD (I)** and **POXD (T)**, reported in this study exhibited exceptionally low  $E_{\text{LUMOS}}$ ,  $E_{\text{HOMOS}}$  and large energy gaps. The LUMO energy levels are related to the conjugation length and the electron-accepting ability of polymers. For some electron-rich conjugated polymers, reduction peak was hardly observed by electrochemical measurement. Conjugated polymers with longer conjugation length and strong electron-accepting ability exhibit lower LUMO energy levels. **POXD (I)** and **POXD (T)** had lower LUMO energy levels than commonly used electron-transporting materials such as Alq<sub>3</sub> ( $E_{\text{LUMO}} = -3.30$  eV) [41], PBD ( $E_{\text{LUMO}} = -2.4$  eV) [42], *p*-POD ( $E_{\text{LUMO}} = -2.8$  eV) [43], PPy ( $E_{\text{LUMO}} = -2.9$  eV) [44], and PQX ( $E_{\text{LUMO}} = -3.16$  eV) [45]. It indicates that, in addition to oxadiazole, the electron-accepting and planar benzo[*c*]cinnoline structure also helps to lower the LUMO energy level. The HOMO energy levels are also associated with the electron-accepting ability. Conjugated polymers with stronger electron-accepting ability have lower HOMO energy levels. **POXD (I)** and **POXD (T)** also had lower HOMO energy levels than Alq<sub>3</sub> ( $E_{\text{HOMO}} = -5.70$  eV) [41], CN-PPV ( $E_{\text{HOMO}} = -5.63$  eV) [40], PPy ( $E_{\text{HOMO}} = -5.70$  eV) [44], and PQX ( $E_{\text{HOMO}} = -5.74$  eV) [45]. The low  $E_{\text{LUMOS}}$  and  $E_{\text{HOMOS}}$  of **POXD (I)** and **POXD (T)** were attributed to the combined effects of benzo[*c*]cinnoline and oxadiazole moieties. These two planar moieties exhibited electron-accepting ability. As show in Fig. 9, the low  $E_{\text{LUMOS}}$  would allow the easier electron injection from air-stable aluminum cathode, and the low  $E_{\text{HOMOS}}$  would block the hole

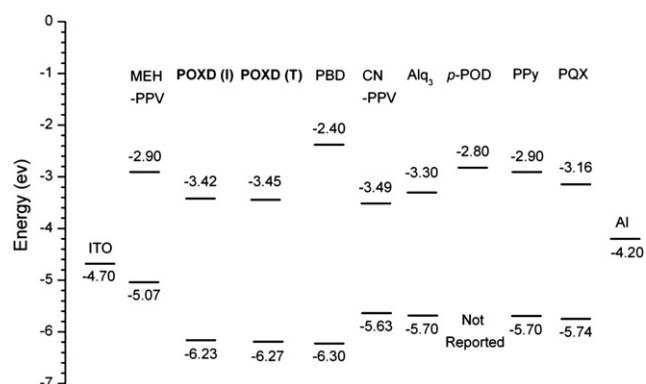


**Fig. 9.** Energy gap diagram.

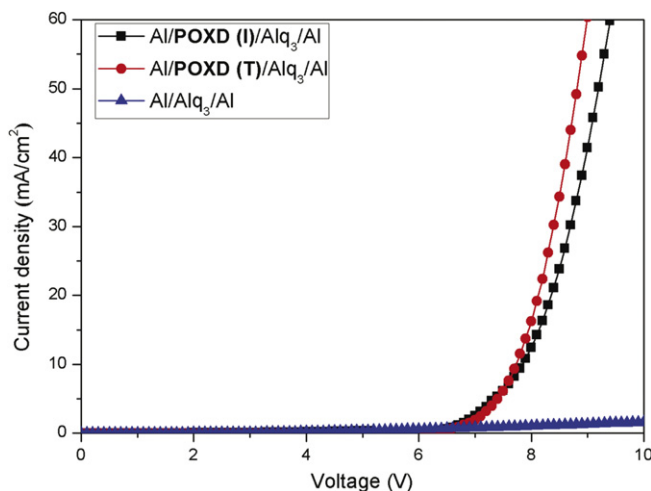


**Fig. 10.** Current density vs. voltage characteristics of electron-only devices.

transported from emitter such as MEH-PPV. In addition, the large band gap should also confine the luminescence in the emitting layers [43].

In order to elucidate the electron-injection and electron-transporting abilities of **POXD (I)** and **POXD (T)**, electron-only devices were fabricated with the structures of Al/**POXD (I)**(150 nm)/Alq<sub>3</sub>(50 nm)/Al, Al/**POXD (T)**(150 nm)/Alq<sub>3</sub>(50 nm)/Al and Al/Alq<sub>3</sub>(200 nm)/Al. Fig. 10 shows the I–V curves of these electron-only devices. It is obvious that the turn-on voltage can be significantly reduced by inserting a layer of **POXD (I)** or **POXD (T)** between the Al and Alq<sub>3</sub>. At a current density of 10 mA/cm<sup>2</sup>, the turn-on voltage of the electron-only devices with a layer of **POXD (I)** or **POXD (T)** was determined to be 7.8 V. No detectable turn-on voltage was observed for the electron-only device without **POXD (I)** or **POXD (T)** layer, indicating the large electron injection barrier from aluminum (4.20 eV) to the LUMO of Alq<sub>3</sub> (3.30 eV). The significant reduction in turn-on voltage can be explained by the lower barriers for electron injection and fast electron-transporting abilities resulted from the electron-accepting benzo[*c*]cinnoline and oxadiazole moieties [46]. Combined with the good thermal stability, benzo[*c*]cinnoline-containing polyoxadiazole **POXD (I)** and **POXD (T)** can be promising candidates for electron-transporting and electron-blocking materials for OLED applications.

#### 4. Conclusions

A four-step synthetic route have been successfully developed to prepare 3,8-benzo[*c*]cinnoline dicarboxylic acid. Polyoxadiazoles **POXD (I)** and **POXD (T)** were prepared by direct polycondensation of this diacid and dihydrazides to form their polyhydrazide precursors **PHA (I)** and **PHA (T)**, followed by thermal cyclodehydration. **PHA (I)** and **PHA (T)** were soluble in polar solvents, while **POXD (I)** and **POXD (T)** polyoxadiazoles were only soluble in concentrated sulfuric acid. These polymers all exhibited good thermal stability. From CV measurements, two reduction peaks were observed for **POXD (I)** and **POXD (T)**, respectively. The results of molecular simulation and CV measurements suggested that the first reduction peaks was resulted from oxadiazole and the second peak was from benzo[*c*]cinnoline. We concluded that oxadiazole moiety had stronger electron affinity than benzo[*c*]cinnoline moiety. **POXD (I)** and **POXD (T)** also exhibited low  $E_{\text{LUMOS}}$  and low  $E_{\text{HOMOS}}$  due to the electron-accepting ability of planar oxadiazole and benzo[*c*]cinnoline as well. These polymers can be promising candidates as the hole-blocking or electron-injection layer for OLED

applications. After appropriate functionalization, the electron-accepting benzo[c]cinnoline moiety can be copolymerized with other electron-rich moieties to adjust the energy levels and charge mobility for various applications.

## Appendix. Supplementary data

Supplementary data associated with this article can be found, in the online version, at doi:10.1016/j.polymer.2011.10.059.

## References

- [1] Akcelrud L. *Prog Polym Sci* 2003;28(6):875–962.
- [2] Shu CF, Dodda R, Wu FI, Liu MS, Jen AKY. *Macromolecules* 2003;36(18):6698–703.
- [3] Chuang CY, Shih PI, Chien CH, Wu FI, Shu CF. *Macromolecules* 2007;40(2):247–52.
- [4] Herguth P, Jiang X, Liu MS, Jen AKY. *Macromolecules* 2002;35(16):6094–100.
- [5] Beaupré S, Boudreault PLT, Leclerc M. *Adv Mater* 2010;22(8):E6–27.
- [6] Blouin N, Michaud A, Gendron D, Wakim S, Blair E, Neagu-Plesu R, et al. *J Am Chem Soc* 2008;130(2):732–42.
- [7] Qin R, Li W, Li C, Du C, Veit C, Schleiermacher HF, et al. *J Am Chem Soc* 2009;131(41):14612–3.
- [8] Slooff LH, Veenstra SC, Kroon JM, Moet DJD, Sweelssen J, Koetse MM. *Appl Phys Lett* 2007;90(14):143506.
- [9] Choi MC, Kim Y, Ha CS. *Prog Polym Sci* 2008;33(6):581–630.
- [10] Curtis MD. *Macromolecules* 2001;34(22):7905–10.
- [11] Yang Y, Pei Q, Heeger AJ. *Synth Met* 1996;78(3):263–7.
- [12] Berggren M, Inganäs O, Gustafsson G, Rasmussen J, Andersson MR, Hjertberg T, et al. *Nature* 1994;372(6505):444–6.
- [13] Pei Q, Yang Y. *J Am Chem Soc* 1996;118(31):7416–7.
- [14] Gustafsson G, Cao Y, Treacy GM, Klavetter F, Colaneri N, Heeger AJ. *Nature* 1992;357(6378):477–9.
- [15] Yu G, Gao J, Hummelen JC, Wudl F, Heeger AJ. *Science* 1995;270(5243):1789–91.
- [16] Strukelj M, Papadimitrakopoulos F, Miller TM, Rothberg LJ. *Science* 1995;267(5206):1969–72.
- [17] Tonzola CJ, Alam MM, Jenekhe SA. *Adv Mater* 2002;14(15):1086–90.
- [18] Lindgren LJ, Zhang F, Andersson M, Barrau S, Hellström S, Mammo W, et al. *Chem Mater* 2009;21(15):3491–502.
- [19] Zhang F, Mammo W, Andersson LM, Admassie S, Andersson MR, Inganäs O. *Adv Mater* 2006;18(16):2169–73.
- [20] Zhang F, Bijleveld J, Perzon E, Tvingstedt K, Barrau S, Inganäs O, et al. *J Mater Chem* 2008;18(45):5468–74.
- [21] Liu SP, Chan HSO, Ng SC. *J Polym Sci Part A Polym Chem* 2004;42(19):4792–801.
- [22] Thompson BC, Kim YG, McCarley TD, Reynolds JR. *J Am Chem Soc* 2006;128(39):12714–25.
- [23] Mikroyannidis JA, Gibbons KM, Kulkarni AP, Jenekhe SA. *Macromolecules* 2008;41(3):663–74.
- [24] Chen JC, Chiang CJ, Liu YC. *Synth Met* 2010;160(17–18):1953–61.
- [25] Adachi C, Tsutsui T, Saito S. *Appl Phys Lett* 1990;56(9):799–801.
- [26] Meng H, Yu WL, Huang W. *Macromolecules* 1999;32(26):8841–7.
- [27] Lee YZ, Chen X, Chen SA, Wei PK, Fann WS. *J Am Chem Soc* 2001;123(10):2296–307.
- [28] Hwang SW, Chen Y. *Macromolecules* 2002;35(14):5438–43.
- [29] Shao X, Luo X, Hu X, Wu K. *J Phys Chem B* 2006;110(31):15393–402.
- [30] Sienkowska MJ, Farrar JM, Zhang F, Kusuma S, Heiney PA, Kaszynski P. *J Mater Chem* 2007;17(14):1399–411.
- [31] Bacon RGR, Pande SG. *J Chem Soc C* 1970;(14):1967–73.
- [32] Patrick DA, Boykin DW, Wilson WD, Tanious FA, Szychala J, Bender BC, et al. *Eur J Med Chem* 1997;32(10):781–93.
- [33] Joshua CP, Philai VNR. *Tetrahedron* 1974;30(18):3333–7.
- [34] Corbett JF, Holt JF. *J Chem Soc*; 1961:5029–37.
- [35] Bjørsvik HR, González RR, Liguori L. *J Org Chem* 2004;69(22):7720–7.
- [36] Yamazaki N, Matsumoto M, Higashi F. *J Polym Sci Part A Polym Chem* 1975;13(4):1373–80.
- [37] Hsiao SH, He MH. *Macromol Chem Phys* 2001;202(18):3579–89.
- [38] Hsiao SH, Chiou JH. *J Polym Sci Part A Polym Chem* 2001;39(13):2271–86.
- [39] Yasuda T, Imase T, Yamamoto T. *Macromolecules* 2005;38(17):7378–85.
- [40] Li Y, Cao J, Gao J, Wang D, Yu G, Heeger AJ. *Synth Met* 1999;99(3):243–8.
- [41] Destruel P, Jolinat P, Clergereaux R, Farenc J. *J Appl Phys* 1999;85(1):397–400.
- [42] Pommerehne J, Vestweber H, Guss W, Mahrt RF, Bässler H, Porsch M, et al. *Adv Mater* 1995;7(6):551–4.
- [43] Kulkarni AP, Tonzola CJ, Babel A, Jenekhe SA. *Chem Mater* 2004;16(23):4556–73.
- [44] Hwang MY, Hua MY, Chen SA. *Polymer* 1999;40(11):3233–5.
- [45] Yamamoto T, Sugiyama K, Kushida T, Inoue T, Kanbara T. *J Am Chem Soc* 1996;118(16):3930–7.
- [46] Lee CC, Chang MY, Huang PT, Chen YC, Chang Y, Liu SW. *J Appl Phys* 2007;101(11):114501.